

# Primordial Black Hole Seeding from Hybrid Inflation - the Direct Integration Approach

by

Alexis Giguere

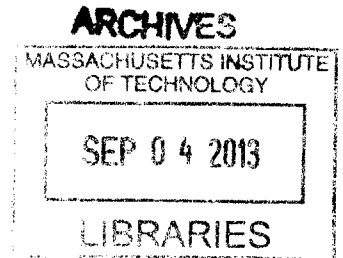
Submitted to the Department of Physics  
in partial fulfillment of the requirements for the degree of

Bachelor of Science in Physics

at the

MASSACHUSETTS INSTITUTE OF TECHNOLOGY

June 2013



© Massachusetts Institute of Technology 2013. All rights reserved.

**Signature redacted**

Author .....

Department of Physics

May 10, 2013

**Signature redacted**

Certified by .....

Alan H. Guth

Professor

Thesis Supervisor

**Signature redacted**

Accepted by .....

Nergis Mavalvala

Senior Thesis Coordinator, Department of Physics



# Primordial Black Hole Seeding from Hybrid Inflation - the Direct Integration Approach

by

Alexis Giguere

Submitted to the Department of Physics  
on May 10, 2013, in partial fulfillment of the  
requirements for the degree of  
Bachelor of Science in Physics

## Abstract

We examine the notion that supermassive black holes at the centre of galaxies, such as the Milky Way, could have been seeded in the early universe by the mechanisms of hybrid inflation. Using luminosity data, we estimate the current density of supermassive black hole. We develop the formalism of the direct integration method in hybrid inflation and obtain a power spectrum, which we try to relate to the literature. Our results do not directly show the plausibility of seeding supermassive black holes, but the shape of the power spectrum suggests that further work might yield positive results.

Thesis Supervisor: Alan H. Guth  
Title: Professor



## Acknowledgments

The author would like to thank Alan Guth for his patience dealing with the endless barrage of emails sent to him while attempting to tackle this difficult subject, as well as Evangelos Sfakianakis, Illan Halpern, and Matthew Joss for their immeasurable contributions.



# Contents

<b>1</b>	<b>Introduction</b>	<b>11</b>
1.1	Black Hole Foundations . . . . .	13
1.1.1	Just How Many Supermassive Black Holes Are There? . . . . .	13
1.1.2	Gravity Preliminaries . . . . .	14
1.1.3	General Relativity and Schwarzschild's Solution . . . . .	15
1.1.4	Simplified Stellar Structure . . . . .	17
<b>2</b>	<b>Inflation as a Formalism of the Early Universe</b>	<b>23</b>
2.1	Inflation Preliminaries . . . . .	23
2.2	Alan Guth's Favorite 3 Problems; Initial Conditions in the Early Universe	24
2.2.1	Horizon Problem . . . . .	25
2.2.2	Flatness Problem . . . . .	25
2.2.3	The Monopole Problem . . . . .	27
2.3	Inflation . . . . .	29
2.3.1	Hydrodynamics Introduction . . . . .	29
2.3.2	Scalar Fields as Drivers of Inflation and Slow Roll . . . . .	31
<b>3</b>	<b>Hybrid Inflation and Seeding</b>	<b>33</b>
3.1	Hybrid Inflation . . . . .	33
3.1.1	Hybrid Inflation Preliminaries . . . . .	33
3.1.2	Hybrid Inflation Dynamics . . . . .	34
3.1.3	Mode Expansion . . . . .	35
3.2	Perturbations . . . . .	38

3.2.1	Time Delay Formalism . . . . .	38
3.2.2	Direct Integration Method . . . . .	39
3.2.3	Results . . . . .	42



# List of Figures

- 3-1 Mode functions  $R$  as a function of e-fold number, taking  $\mu_\phi = 18$  and  $\mu_\psi = 1/18$ . The pale blue is for  $k = 256$ , the green is for  $k = 64$ , the gray for  $k = 1$ , the red for  $k = 1/64$ , and dark blue for  $k = 1/256$ . . . 37
- 3-2 This plot was adapted, with permission, from a plot produced by Evangelos Sfakianakis. Graphed is the  $\tau$  spectrum, as a function of  $k$  in Hubble units. Note the presence of a peak at around  $k = 10$ . . . . . 43



# Chapter 1

## Introduction

From our perspective, centered on our small planet, the world outside our atmosphere is vast and puzzling. Large expanses of space separate us from even the closest structure, and for most of our history it was assumed that the realm of the stars was divine and unreachable. This isolation, however, is broken by the propagation of light.

Much of what we know about the Universe now is based on the behavior of electromagnetic waves. Classical electromagnetism helped Albert Einstein formulate his theory of relativity in 1915. General relativity pioneers, such as Schwarzschild and Droste, realized that Einstein's equations naturally lent themselves to the possibility of curvature singularities; these would come to be known as black holes. Chandrasekhar and Oppenheimer showed that neutron stars above a certain mass would necessarily collapse into singularities, thereby legitimizing black holes as astrophysical objects.

But are black holes relegated to near solar-mass sizes? The early formalism proposed by Schwarzschild spoke of the mass density required for collapse, but no mention was made of mass scale. Clearly, if all black holes are to result from stellar collapse, then the spectrum of their masses is limited by the weak spread of main sequence masses.

Another perspective was proposed by Martin Rees in 1971. Using ultraviolet data from the National Radio Astronomy Observatory (NRAO), he asserted the possibility

that the Milky Way galactic center contained enough mass, in a sufficiently small volume, to form a black hole. The novelty of the idea, however, was the mass scale he proposed. The supermassive black hole had to be at least 5 orders of magnitude heavier than a typical stellar black hole in order to account for the large Doppler spread of water masers around the galactic center. The idea rapidly caught on, and resources were invested towards identifying near center objects in an attempt to better understand the mass constituents of the center.

The most convincing argument for the presence of a supermassive black hole in the center of the Milky Way came in 2002 when astronomers, working with data from the Very Large Telescope (VLT) at the European Observatory in Chile, measured stellar velocities and X-ray emission of nearby stars. They showed that the mass concentration near Sagittarius A\* was not a cluster of astrophysical objects or massive, degenerate fermions, but rather a strongly constrained central density. Thus came wide-spread acceptance of the presence of supermassive black holes not only at the center of the Milky Way, but also of other spiral-type galaxies.

While most of the work has been done in terms of characterizing the properties of supermassive black holes, the question of origins remains. Ordinary stellar black holes provide us with a relatively straightforward narrative. Large stars collapse into neutron stars, which then may collapse into black holes if their mass is large enough. Our understanding of stellar black holes is tied to our understanding of stellar evolution, which is believed to be known fairly accurately. But supermassive black holes provide no such obvious narrative. The gap between stellar black holes, for whom the mass upper bound is believed to be of order 10 Solar Masses, and the observed supermassive black holes, whose masses are believed to range in the millions of Solar Masses, is roughly 5 order of magnitude, suggesting that the processes leading to their formation are probably different. This paper will attempt to show the plausibility of seeding supermassive black holes in the very early universe using inflationary cosmology, and discuss the inflation density perturbations required to possibly achieve primordial black holes. The difficulty of this task will be explained.

## 1.1 Black Hole Foundations

### 1.1.1 Just How Many Supermassive Black Holes Are There?

According to astronomer Paul Schechter, the modern understanding of active galactic nuclei has progressed sufficiently that we are fairly confident of their concomitance with supermassive black holes. This means that we can, naively, estimate the number density of supermassive black holes as roughly 1 per galaxy. Just how many is that, however? To address this question, we propose to use the Schechter luminosity function.

The Schechter function  $\phi_{\bar{x}}(L)$  is the number of galaxies in a given region per unit volume per unit luminosity. This function varies depending on which region is observed, but over large scales (i.e. larger than 100 Mpc), the space-dependence goes away, and we now have a universal function  $\phi(L)$ .

By fitting to experimental data, Schechter[1] found  $\phi(L) = \left(\frac{\phi^*}{L^*}\right) \left(\frac{L}{L^*}\right)^\alpha e^{-L/L^*}$ , where  $\alpha \approx -1.07$ ,  $\phi^* \approx 0.04 \text{ Mpc}^{-3}$ , and  $L^* \approx 2.3 \times 10^{10} L_\odot$ .

To obtain the number density of galaxies  $n_g$ , we first find the luminosity density by integrating

$$\begin{aligned} n_l &= \int_L^\infty L' \phi(L') dL' \\ &= \phi^* L^* \int_{L/L^*}^\infty \left(\frac{L'}{L^*}\right)^{\alpha+1} e^{-L'/L^*} d\left(\frac{L'}{L^*}\right), \end{aligned} \quad (1.1)$$

where  $L \ll L^*$  is the minimum luminosity. We have written the integrand suggestively, so as to use the fact that we know elementary calculus that

$$\int_0^\infty x^{\alpha-1} e^{-x} dx = \Gamma(\alpha), \quad (1.2)$$

where  $\Gamma(\alpha)$  is the Gamma function. We can then rewrite the limits of integration

and get

$$\begin{aligned}
n_l &= \phi^* L^* [\Gamma(\lambda + 2) - \Gamma(L/L^*)] \\
&\approx \phi^* L^* [\Gamma(1) - \Gamma(0)] \\
&\approx \phi^* L^* \\
&\approx 9.2 \times 10^8 L_\odot \text{Mpc}^{-3}.
\end{aligned} \tag{1.3}$$

If the universe were comprised of Milky Ways, in other words if the Milky Way luminosity were representative, then we would find the number density by dividing the luminosity density by the luminosity of a the Milky Way:

$$n_g = \frac{9.2 \times 10^8 L_\odot \text{Mpc}^{-3}}{1.7 \times 10^{10} L_\odot} \approx 0.05 \text{Mpc}^{-3}. \tag{1.4}$$

Assuming at least a 1-to-1 ratio of supermassive black hole to galaxy, we obtain a similar number density for the black holes.

This current day density is interesting, but all sorts of phenomena could have occurred to chance it from the time primordial black holes were seeded to now. Furthermore, without knowing exactly when the black holes were seeded, we are limited in the actual numerical comparisons we can make. More about this in chapter 3.

### 1.1.2 Gravity Preliminaries

Eintsein's mathematical description of gravity marks a departure from the Newtonian paradigm. There is no direct expression for the gravitational force between objects. Instead, the paradigm shifts to the energy-momentum content of space and the way it influences its geometry. General Relativity, the end product theory, is based on Riemannian geometry, and next we summarize some of it.

Spacetime, or the set of space and time coordinates, is taken to be a metric space, namely an ordered pair  $(X, d)$  where  $X$  is a set with a Cartesian product  $X \times X = \{(x, y) : x, y \in X\}$  and  $d$  is a *metric*. The metric becomes the defining aspect of the space; two spaces with the same metric are identical. Now, what

characteristics do we need this metric to have? Intuitively, we want it to allow us to calculate distances, so a few things come to mind. First, it should be non-negative. It should also follow the coincidence axiom, namely that the distance between two points should be zero if and only if these two points are identical. It should be symmetric too, since we want the distance between points  $x$  and  $y$  to be equivalent to the distance between  $y$  and  $x$ . Finally, we would like our notion of distance to follow the triangle inequality, since we like to be able to insist on convergence properties (such as in a Hilbert space).

We can now put together these four ideas more formally as follows. A metric is defined as a mapping  $d : X \times X \mapsto \mathbb{R}$  such that, for all  $x, y, z \in X$ :

- (i)  $d(x, y) = d(y, x)$
- (ii)  $d(x, y) \geq 0$
- (iii)  $d(x, y) = 0 \iff x = y$ , and
- (iv)  $d(x, z) \leq d(x, y) + d(y, z)$ .

We can now attempt to describe the geometry of spacetime uniquely in terms of the metric. Specifically, spacetime is represented as a 4-dimensional differentiable manifold and, using the four conditions mentioned above (as well as local Lorentz covariance), a covariant, second-rank, symmetric tensor  $g_{\mu\nu}$  on the manifold.

### 1.1.3 General Relativity and Schwarzschild's Solution

As stated in the previous section, Einstein's 1915 epiphany was to treat gravitational forces as a consequence of energy-momentum affecting the metric tensor. His work produced the famous field equations, which take the form

$$R_{\mu\nu} - \frac{1}{2}Rg_{\mu\nu} = T_{\mu\nu}, \tag{1.5}$$

where  $R_{\mu\nu\sigma\rho}$  is the Riemann curvature tensor and  $T_{\mu\nu}$  is the energy-momentum tensor. This simplicity of form is misleading, however, because "hidden" into  $R_{\mu\nu\sigma\rho}$  are non-

linear second-order derivatives of the metric. Analytical solutions are hard to come by, but thankfully for us, the simplest of solutions is sufficient to begin understanding black holes.

Shortly after the publication of the field equations, Schwarzschild found a solution for the case of a spherically-symmetric, uncharged, non-rotated mass  $M$ . The resulting geometry, named the Schwarzschild metric, is written in spherical  $(t, r, \theta, \phi)$  coordinates as

$$ds^2 = - \left(1 - \frac{2GM}{r}\right) dt^2 + \left(1 - \frac{2GM}{r}\right)^{-1} dr^2 + r^2(d\theta^2 + \sin^2\theta d\phi^2). \quad (1.6)$$

At first glance, this geometry looks dangerously singular at  $r = 2M$  (let's take  $G = 1$ ). It is easy to show, however, that the danger is in fact benign. Consider an "astronaut" coming in from far away, where the metric is incidentally flat. Assume the astronaut is coming in freely and radially. We can calculate his trajectory, a radial geodesic, through spacetime and find that his coordinate time is given by

$$\frac{t}{2M} = -\frac{2}{3} \left(\frac{r}{2M}\right)^{3/2} - 2 \left(\frac{r}{2M}\right)^{1/2} + \ln \left| \frac{(r/2M)^{1/2} + 1}{(r/2M)^{1/2} - 1} \right| + \text{constant}, \quad (1.7)$$

which tell us that the astronaut needs an infinite lapse in coordinate time to reach  $r = 2M$ . However, coordinate time isn't relevant to the astronaut's experience; only proper time  $\tau$  is. But  $\tau$  isn't behaving singularly at  $r = 2M$ :

$$\frac{\tau}{2M} = -\frac{2}{3} \left(\frac{r}{2M}\right)^{3/2} + \text{constant}. \quad (1.8)$$

So the astronaut reaches the  $r = 2M$  in finite time on his watch. We can further show that the tidal forces felt by the astronaut at the specified radius are finite too, since the components of the Riemann tensor are finite. Cranking through the algebra in the astronaut's frame, we find that every component of the Riemann tensor vanish,



except

$$R_{\hat{t}\hat{r}\hat{t}\hat{r}} = -\frac{2M}{r^3} \qquad R_{\hat{t}\hat{\theta}\hat{t}\hat{\theta}} = R_{\hat{t}\hat{\phi}\hat{t}\hat{\phi}} = \frac{M}{r^3} \qquad (1.9)$$

$$R_{\hat{\theta}\hat{\phi}\hat{\theta}\hat{\phi}} = \frac{2M}{r^3} \qquad R_{\hat{r}\hat{\phi}\hat{r}\hat{\phi}} = R_{\hat{r}\hat{\theta}\hat{r}\hat{\theta}} = \frac{-M}{r^3}. \qquad (1.10)$$

Tidal forces are finite everywhere, except for  $r = 0$ . For good measure, we can calculate the invariant Kretschmann scalar  $K \equiv R_{\mu\nu\sigma\rho}R^{\mu\nu\sigma\rho} = 48M^2/r^6$  and conclude that in every local Lorentz frame, including the astronaut's, tidal forces will become infinite at  $r \rightarrow 0$ .

While we have shown that there is no obvious “pathology” happening at  $r = 2M$ , this does not mean that nothing interesting happens there. In fact, a crucial turnaround occurs with timelike and spacelike coordinates. In the region  $r > 2M$ , the  $t$  direction ( $\partial/\partial t$ ) is timelike since  $g_{tt} > 0$  and the  $r$  direction is spacelike. However, when  $r < 2M$ ,  $g_{tt}$  and  $g_{rr}$  switch signs.

What does this mean? Prior to crossing the Schwarzschild radius, the astronaut is in control of his  $r$  coordinate, but not of  $t$ . He can move back and forth in  $r$ , but time goes forward inexorably. When he crosses the horizon, however, things change. A decrease in “ $r$ ” represents the “passage of time”, strictly forward-going. This means that, as inexorable as the passage of time for an ordinary astronaut well outside of the horizon, the spacetime path of anybody within  $r = 2M$  will lead to  $r \rightarrow 0$ . It is this condition, in the words of Stephen Hawking (as reported by Kip Thorne in *Warping Spacetime*), that defines a black hole.

### 1.1.4 Simplified Stellar Structure

The next logical question to ask (other than what happens at  $r = 0$ , but that one is harder to pin down) is perhaps one of genesis: where do black holes come from? At first pass, any mass  $M$  will have a Schwarzschild radius  $r = 2GM$ . But point masses are not observed experimentally, so any mass  $M$  will have some spacial extent and therefore a mass density. Will these densities necessarily collapse in to form black holes? Of course they will not, for objects in the universe are more than simple

gravitational puppets. Pressure, be it thermal or degeneracy, will antagonistically fight gravitational collapse and reach a dynamical equilibrium. Our investigation of black holes, then, means understanding when pressure is insufficient to counteract gravity.

This qualitative discussion can be made quantitative in the case of stars. Stars are, after all, important astrophysical objects. They are the important constituents of galaxies that also provide an observational footprint. More importantly, they are objects whose constituents we can guess with reasonable certainty. The following discussion is adapted from Paul Schechter's 2013 Modern Astrophysics class.

Ignoring stellar rotation, magnetic fields, time-dependent composition changes, and strong luminosity variability (as in Cepheid variables), we can model basic stellar structure. Assuming spherical symmetry and a power-law relationship between pressure and density ( $P = \kappa \rho^{(n+1)/n}$ , where  $n$  is called the polytropic index and  $\kappa$  is a constant) we can differentiate the equation of hydrostatic equilibrium to obtain the dimensionless Lane-Emden equation

$$\frac{1}{\xi^2} \frac{d}{d\xi} \xi^2 \frac{d}{d\xi} \phi = -\phi^n, \quad (1.11)$$

where  $\xi \equiv r \left( \frac{\kappa(n+1)\lambda^{1/n-1}}{4\pi G} \right)^{-1/2} = r/a$  is the dimensionless radius and  $\rho = \lambda \phi^n$  defines the dimensionless density. The total physical radius of the star  $r_{max} = a\xi_{max}$  corresponds to the largest  $\xi$  for which the dimensionless density is greater than 0. We can then compute the mass enclosed in the star by integrating the density:

$$\begin{aligned} M &= \int_0^{r_{max}} 4\pi r^2 \rho dr \\ &= 4\pi \lambda a^3 \int_0^{\xi_{max}} \phi^n \xi^2 d\xi. \end{aligned} \quad (1.12)$$

Now we can use the Lane-Emden equation to substitute for  $\phi$  and get that

$$M = -4\pi\lambda a^3 \int_0^{\xi_{max}} \frac{d}{d\xi} \left( \xi^2 \frac{d\phi}{d\xi} \right) d\xi, \quad (1.13)$$

which begs for the use of the fundamental theorem of calculus. By looking at hydrostatic equilibrium, we conclude that  $\frac{d\phi}{d\xi} \Big|_{\xi=0} = 0$ . Putting it together with (1.9), we obtain

$$\begin{aligned} M &= -4\pi\lambda a^3 \xi^2 \frac{d\phi}{d\xi} \Big|_0^{\xi_{max}} \\ &= -4\pi\lambda a^3 \xi^2 \frac{d\phi}{d\xi} \Big|_{\xi_{max}}. \end{aligned} \quad (1.14)$$

This expression is in terms of the  $\xi_{max}$  and the slope of  $\phi$  at  $\xi_{max}$ , which are dimensionless quantities that can be calculated by solving numerically the Lane-Emden equation for a given polytropic index. However, we still have to find a central density  $\lambda$  and an  $a(\kappa)$  in order to get an idea of the behavior of the mass of simplified stars. To do so, we make a small interlude into statistical mechanics.

## Equation of State for White Dwarfs

White dwarfs are interesting candidates as intermediaries towards black holes. How can we adapt what we know of degenerate white dwarfs to the ideas proposed in the previous section?

The first step involves writing a general expression for the pressure in a degenerate neutron star. Using suggestions from Paul Schechter, we write the pressure as

$$P = \int_0^{\pi/2} d\theta \int_0^{\infty} f(p) (2\pi p^2 \sin \theta) (v \cos \theta) (2p \cos \theta) dp, \quad (1.15)$$

where  $f(p)$  is the phase space density, the second bracketed term corresponds to the “velocity flux” and the third bracketed term is the momentum transfer. For a Fermi-Dirac distribution at temperature  $T = 0$ , the phase space density simplifies to  $g/h^3$  for  $p < p_f$ , where  $p_f$  is the Fermi momentum and  $g$  is the number of spin states (we

take it to be 2), and 0 otherwise.

Assuming that our degenerate neutron star is highly relativistic, we perform the integral by rewriting  $v = \frac{p/m_e}{\sqrt{1+(p/m_e c)^2}}$  and letting  $x \equiv p/m_e c$ :

$$P = \frac{8\pi m_e^4 c^5}{3h^3} \int_0^{p_f/m_e c} \frac{x^4}{\sqrt{1+x^2}} dx. \quad (1.16)$$

In the ultra-relativistic range,  $x \gg 1$ , so the integral simplifies to

$$\begin{aligned} P &= \frac{8\pi m_e^4 c^5}{3h^3} \int_0^{p_f/m_e c} x^3 dx \\ &= \frac{8\pi c}{12h^3} p_f^4. \end{aligned} \quad (1.17)$$

To find an expression for  $p_f$ , we integrate the phase space density:

$$\begin{aligned} n_e &= \int_0^{p_f} 4\pi p^2 f(p) dp \\ &= \frac{8\pi}{3h^3} p_f^3, \end{aligned} \quad (1.18)$$

where  $n_e$  is the number density of electrons. Finally, we use the fact that  $n_e = \frac{\rho}{\mu_e m_p}$ , where  $\mu_e$  is the fractional ‘‘molecular weight’’, in units of proton, of the electron and  $m_p$  is the proton mass, to obtain

$$P = \frac{hc}{8} \left( \frac{3}{\pi \mu_e^4 m_p^4} \right)^{1/3} \rho^{4/3}. \quad (1.19)$$

This is the result we needed. Referring back to the polytropic equation of state, we can now kill two birds with one equation (we promise to eat the birds afterward). First, the power-law dependence of (1.15) tells us that  $n = 3$  in (1.7). Furthermore, the coefficients suggest that  $\kappa = \frac{hc}{8} \left( \frac{3}{\pi} \right)^{1/3} (\mu_e m_p)^{-4/3}$ .

Going back to (1.10), we substitute for  $a$  and find that the dependence on the central density  $\lambda$  vanishes. We can rewrite it in a suggestive way:

$$M = - \left[ \frac{1}{\pi} \left( \frac{hc}{2Gm_p^2} \right)^{3/2} \left( \frac{3}{4} \right)^{1/2} \mu_e^{-2} \xi_{max}^2 \frac{d\phi}{d\xi} \Big|_{\xi_{max}} \right] m_p, \quad (1.20)$$

which numerically evaluates to  $M_c = \frac{5.8}{\mu_e^2} M_\odot \approx 1.45 M_\odot$  for an electron mean molecular weight of 2, where we have taken the liberty of labeling our radius-independent mass  $M_c$  in honor of Chandrasekhar.

This result tells us that a spherically-symmetric, non-rotating, non-varying, non-magnetic white dwarf cannot be in equilibrium (i.e. stable) if it is any more massive than  $M_c$ . Our result, which is based on heavy simplifications, is still in close agreement with the accepted value for the Chandrasekhar limit, which is  $1.44 M_\odot$  [2].

While we have not shown that stars do indeed collapse into black holes, we have provided an illustration of the tug-of-war between gravity and pressure in astrophysically-significant objects.

Could supermassive black holes result from the collapse of dying stars? It seems unlikely, given the very large masses involved. Where then? In the next section and beyond, we will look at possible early universe scenarios, and attempt to relate our understanding of the dynamics to the seeding of primordial black holes as precursors of supermassive black holes.



## Chapter 2

# Inflation as a Formalism of the Early Universe

### 2.1 Inflation Preliminaries

Generally speaking, the further away from us a phenomenon is, the harder it is to understand. The very early universe, where presumably large energy scales reigned supreme, is an example of a time so remote that it is difficult for physicists to reach a high level certainty as to what was really going on then. Nevertheless, the current universe is kind enough to offer some clues. In particular, our understanding of the universe involves two central principles. These principles, while rich in consequences, are simple to explain.

First, we will take for granted that over distances larger than 100 Mpc, the universe is homogeneous. This assumption is, no pun intended, rather weighty and deserves a bit of attention. Indeed, it is rather clear that the universe is not homogeneous on small distance scales. The Milky Way galaxy, for instance, comprises of a disk of about 100 000 light-years with a bulge centered around the center of the disk. Go 100 000 lights years away from the center, directly up following the rotational axis of the disk, however, and you will find a mass density many orders of magnitude smaller than the average mass density of the galaxy[3].

On the scale of galaxy superclusters, however, things are much smoother. Data[?]

shows that the space between superclusters does not vary significantly, and so spheres of radius 100 Mpc all contain, more or less, the same mass.

The second assumption we make is isotropy, which says means that there are no preferred direction in the universe. Like in the case of homogeneity, isotropy only holds for distances over the supercluster size, namely 100 Mpc. In other words, an astronomer observing the universe 100 Mpc away would see exactly the same thing regardless of the direction in which the telescope is pointing. When we combine isotropy and homogeneity, we obtain the cosmological principle. Of course, data from the Cosmic Microwave Background (CMB) supports the notion that, at recombination, the universe was extremely homogeneous and isotropic.

Naturally, our investigation of primordial black holes involves structures that are very much inhomogeneous when compared to the background. So any understanding of early universe physics has to, in one fell swoop, address both homogeneity and isotropy, while at the same time offer an avenue to “seed” inhomogeneities. This is a challenge, and in the next section we propose to discuss the initial condition problems we face. Problems are made to be solved, however, and posing the problems leads us to a solution, namely inflation, a version of which we will use to tackle the primordial black hole problem.

## **2.2 Alan Guth’s Favorite 3 Problems; Initial Conditions in the Early Universe**

Generally speaking again, there are two independent sets of initial conditions characterizing matter: the spacial distribution, which is described by an energy density, and the initial field of velocities. What can we say about them, given the current state of the universe?



### 2.2.1 Horizon Problem

First, let's examine the fact that the universe is nearly homogeneous and isotropic on very large distance scales. The following discussion mirrors a lecture given by Alan Guth in the Early Universe course. Take the present horizon scale to be of order  $ct_0 = (3 \times 10^{10} \text{m/s})(13.75 \text{Gyr}) \sim 10^{26} \text{ m}$ . The size of the homogeneous and isotropic region, at an earlier time denoted by the subscript  $i$ , is therefore at least as large as  $d_i \sim ct_0 \frac{a_i}{a_0}$ , where  $a$  corresponds to the scale factor.

Now, let us compare this distance to the size  $d_c \sim ct_i$  of a causal region. Taking ratios, we have

$$\frac{d_i}{d_c} \sim \frac{t_0 a_i}{t_i a_0}. \quad (2.1)$$

While we cannot know exactly what value this ratio takes, we do know that at temperatures greater than the Planck temperatures  $T_P$  we enter the realm of quantum gravity, and that primordial radiation dominates at the Planck time  $T_P$ . We can estimate the ratio of the scale factors as the inverse ratios of the temperatures in the following manner:

$$\frac{a_i}{a_0} \sim \frac{T_0}{T_P} \sim (2.75) \left( \frac{\hbar c^5}{k^2 G} \right)^{-1/2} \sim 10^{-32} \quad (2.2)$$

Using the Planck time, we get

$$\frac{d_i}{d_c} \sim 10^{28}. \quad (2.3)$$

Assuming that no signal can propagate faster than the speed of light, this is a strange result. At the Planck time, the size of the homogeneous universe was roughly 28 orders of magnitude bigger than the causality scale. In the words of Barbara Ryden, on page 194 of her book *Introduction to Cosmology*, "how can two points that haven't had time to swap information be so nearly identical?"

### 2.2.2 Flatness Problem

We have discussed, after a fashion, the matter distribution. Now let us address the velocities, more specifically how incredibly accurately they must be set so that the negative gravitational energies of matter be compensated.

We assume Hubble expansion, so that the initial homogeneity not be quickly destroyed. Consider a spherically symmetric cloud of stuff. We can compare its total energy  $E_{tot}$  to its kinetic energy due to Hubble expansion  $E_H$ . We further assume that the only interaction between constituents comes as the result of gravity, so that the negative potential energy of the gravitational self-interaction is given by  $E_G$ . By conservation, we have

$$E_{tot} = E_H^i + E_G^i = E_H^0 + E_G^0. \quad (2.4)$$

But since  $E_H$  is a kinetic energy, we have  $E_H \sim v^2$ , where  $v$  is the velocity, so we can relate it to the time derivatives of the scale factor:

$$\frac{E_H^i}{E_H^0} = \left( \frac{\dot{a}_i}{\dot{a}_0} \right)^2 \quad (2.5)$$

Taking ratios, we have

$$\frac{E_{tot}^i}{E_H^i} = \frac{E_H^i + E_G^i}{E_H^i} = \frac{E_H^0 + E_G^0}{E_H^0} \left( \frac{\dot{a}_0}{\dot{a}_i} \right)^2. \quad (2.6)$$

Next, we assume that the scale factor grows as some power of time. This may not be right, but it isn't insane, so we move on and estimate that  $\dot{a} \sim a/t$  as polynomials do. We can use (2.1) and (2.3) to rewrite

$$\frac{E_{tot}^i}{E_H^i} \leq \frac{E_H^0 + E_G^0}{E_H^0} (10^{-28})^2. \quad (2.7)$$

We expect the Hubble expansion kinetic energy to be of order of the gravitational energy (up to a negative sign), or at the very least we don't expect it to be many orders of magnitude larger, so we conclude that

$$\frac{E_{tot}^i}{E_H^i} \leq 10^{-56}. \quad (2.8)$$

This result is problematic, as was (2.3). It means that for given energy density distributions, the Hubble velocities must be adjusted extremely finely, to an "accuracy" of  $10^{-54}\%$ .

### 2.2.3 The Monopole Problem

To begin, we admit to having never really understood this topic until we came across notes by Arjen Baarsma while researching this paper. The following discussion is therefore based on Baarsma's 2009 seminar notes from the University of Utrecht, which are available online.

Monopoles arise if the vacuum manifold of the potential has the topology of a two-dimensional sphere. To see how this can work, consider the Higgs mechanism. Its main feature, arguably, is the existence of real  $n$ -plet of scalar fields  $\phi \equiv (\phi^1, \phi^2, \dots, \phi^n)$  used to break the original symmetry of the theory. Their Lagrangian can be written, depending on the model, as

$$\mathcal{L}_\phi = \frac{1}{2} \partial_\mu \phi \partial^\mu \phi - \frac{\lambda}{4} (\phi^2 - \sigma^2)^2. \quad (2.9)$$

At very high temperatures, symmetry is restored and the Higgs field has a vanishing expectation value, or  $\phi = 0$ . As the universe cools below  $T_{GUT}$ , phase transitions take place and the scalar fields acquire vacuum expectation values corresponding to the minimum of the potential in (2.9):

$$\phi^2 = \sum_{i=1}^n \phi_i^2 = \sigma^2. \quad (2.10)$$

Note that if  $n = 3$ , (2.10) manifestly describes  $S^2$ . If we consider two causally disconnected regions  $A$  and  $B$ , we find that with probably  $\mathcal{O}(1)$  we can have  $\phi_A^i > 0$  and  $\phi_B^i < 0$ ,  $i = 1, 2, 3$  and  $\phi^i$  satisfy (2.10). But 3 2-dimensional hypersurfaces determined by  $\phi^i(x^1, x^2, x^3) = 0$  generically cross each other at a point. Since all 3 fields vanish there, this is the point of false vacuum. Thus a monopole, a 0-dimensional topological defect, is created.

Now, the actual probability that the orientation of the Higgs field around the point is topologically non-trivial is, as we have written, close to 1. However, its exact value will depend, as explained in Baarsma, on the shape of the vacuum manifold. It can be estimated by looking at how many of the possible configurations, around a

point, result in monopoles. Taking the vacuum manifold to be the 2-sphere described above, we use Kibble[4] to find a probability  $P \approx 0.1$ . We also take the GUT scale to be roughly  $10^{16}$  GeV, and the horizon to be  $d_{GUT} \sim 8 \times 10^{-28} (T_{GUT}/10^{16}\text{GeV})^{-2}$  cm. So right after the phase transition, the number density  $n_{GUT}$  of monopoles is, at least,

$$n_{GUT} \geq P \cdot d_{GUT}^{-3} \sim 10^{80} (T_{GUT}/10^{16}\text{GeV})^6 \text{cm}^{-3}, \quad (2.11)$$

which is large.

Monopoles, because of their topological nature, cannot decay into other particles. They can, however, annihilate with their companions anti-monopoles and release their total mass-energy in a process that preserves the total topological charge. Perhaps most of the early universe monopoles annihilated, thereby depleting their numbers? Not so fast, said Zeldovich and Khoplov[5]. They proposed that the attractive force between monopoles of opposite charge are of the order of the Coulomb force, allowing them to estimate the rate at which monopoles and anti-monopoles capture each other and annihilate. They found that pair annihilation is a slow and inefficient process, mostly due to the high monopole mass. When the ratio  $n_{GUT}/T^3$  falls under  $10^{-8} (m_{monopole}/10^{17}\text{GeV})$ , annihilation becomes unable to keep up with the expansion of the universe[6]. At this point, the number density must scale as  $a^{-3}$ . Assuming the universe cools down adiabatically afterward, the total entropy is conserved (as per discussions with Alan Guth) and entropy density  $s$  scales as  $a^{-3}$ , telling us that  $n_{GUT}/s$  is conserved. Now, using results from Alan Guth's 8.286 class, we write the entropy density as  $s = g_* \frac{2\pi}{45} T^3$ , where  $g_*$ , the effective number of freedom, is taken to be around 100, as per discussions with Alan Guth. This allows us to obtain the constant

$$n_{GUT}/s \sim 4 \times 10^{-9} (T_{GUT}/10^{16}\text{GeV})^3, \quad (2.12)$$

assuming the initial ratio is smaller than the annihilation threshold and monopole annihilation plays no role. This means that the current monopole number density would be  $n \sim 10^{-7} (T_{GUT}/10^{16}\text{GeV})^3 \text{cm}^{-3}$  today, when  $T = 2.725\text{K}$  and  $g_* = 3.91$ . If the monopole mass is around  $10^{17}\text{GeV}$ , then we get a monopole energy density of

roughly  $10^9$  GeV/cm today. This is 16 orders of magnitude larger than the accepted total energy density of baryonic matter in the universe. Clearly, this cannot be. The universe is not dominated by magnetic monopoles today. In fact, there is no strong evidence that they exist at all.

## 2.3 Inflation

### 2.3.1 Hydrodynamics Introduction

One may be tempted to gloss over the monopole problem as a mere artifact of a deficient grand unified theory, but it is harder to dismiss the flatness and horizon problems. The problem, we recall, is that the ratio  $\dot{a}_i/\dot{a}_0$ , which we found to be very large, determines the number of causally disconnected regions and defines the necessary accuracy of the initial velocities. Now, if gravity was always attractive, we would expect, naively, that  $\dot{a}_i/\dot{a}_0 \gg 1$ , since gravity would slow down expansion. However, what if during some period of expansion gravity acted repulsively? We could have  $\dot{a}_i/\dot{a}_0 < 1$ , and the creation of a single causally-connected domain universe may become possible. Of course, we would still want the successful predictions of the pre-inflation Friedman model, such as nucleosynthesis, to hold. So we would want inflation to begin and end rather quickly.

To see how all this may work, consider the second-order Friedmann equation

$$\ddot{a} = -\frac{4\pi}{3}G(\epsilon + 3P)a, \quad (2.13)$$

where  $\epsilon$  is the energy density and  $P$  the pressure. Accelerated expansion can occur with  $\ddot{a} > 0$  only if  $\epsilon + 3P < 0$ . This latter condition is fine, but it isn't much of an equation of state.

To make progress, we recall that  $\ddot{a}/a = H^2 + \dot{H}$ . At the end of inflation,  $\ddot{a}$  must be negative (to gracefully join up with Friedmann expansion), so  $\dot{H}$  must be negative as well. But  $|\dot{H}|/H^2$  grows towards the end of inflation, which takes place roughly when  $|\dot{H}| = \mathcal{O}(H^2)$ . Assuming  $H^2$  changes faster than  $\dot{H}$ , we get an estimate for the

end of inflation

$$t_{end} \sim H_i/|\dot{H}_i|, \quad (2.14)$$

where the subscript  $i$  refers the “beginning” of inflation.

Inflation, of course, should last long enough to magnify a tiny patch of space to the point where it reaches a scale comparable to the observable universe. Now, CMB data shows that inhomogeneities do not surpass  $10^{-5}$ . Artifacts of a large inhomogeneity, provided

$$\dot{a}_i/\dot{a}_0 < 10^{-5}, \quad (2.15)$$

will be sufficiently diluted. Since  $H = \dot{a}/a$ , we can rewrite (2.15) as

$$\frac{\dot{a}_i}{\dot{a}_{end}} \frac{a_{end}}{a_0} = \frac{a_i}{a_{end}} \frac{H_i}{H_{end}} \frac{a_{end}}{a_0} < 10^{-5}. \quad (2.16)$$

But  $a_{end}/a_0 > 10^{28}$ , and we conclude that we need

$$\frac{a_{end}}{a_i} > 10^{33} \frac{H_i}{H_{end}}. \quad (2.17)$$

Over the course of inflation, we have  $H_i^2 \gg |\dot{H}_i|$ , so we estimate

$$\frac{a_{end}}{a_i} \sim e^{H_i t_{end}} \sim e^{H_i^2/|\dot{H}_i|} > 10^{33}. \quad (2.18)$$

This essentially says that we would like inflation, at least in the most basic terms, to last longer than  $\ln(10^{33}) \approx 76$  Hubble times (or e-folds), in other words  $t_{end} > 76 H_i^{-1}$ .

We use the fact that we can write Friedmann’s equations (taking  $k = 0$ ) as  $H^2 = \frac{8\pi G}{3}\epsilon$  and  $\dot{H} = -4\pi G(\epsilon + P)$ , we reformulate the 76 e-fold condition (which can be expressed as  $|\dot{H}_i|/H_i^2 < 1/76$ ) as

$$\frac{(\epsilon + P)_i}{\epsilon_i} < 10^{-2}. \quad (2.19)$$

This tells us that, at the earliest stages of inflation, a de Sitter solution is rather good, with the deviation not exceeding 1%.

### 2.3.2 Scalar Fields as Drivers of Inflation and Slow Roll

Although the word “scalar” is nowhere to be found in Alan Guth’s seminal 1981 paper, Prof. Guth [7] discovered that scalar fields are natural drivers for inflation.

At first, we note that the energy-momentum tensor for a scalar field can be rewritten in a form similar to that of an idea fluid. The energy density is then

$$\epsilon = \frac{1}{2}\dot{\phi}^2 + V(\phi) \quad (2.20)$$

for a potential  $V(\phi)$ , in a region where  $\phi$  is homogeneous. The pressure is

$$P = \frac{1}{2}\dot{\phi}^2 - V(\phi). \quad (2.21)$$

Since we wish to achieve  $P \approx -\epsilon$  (refer to previous section), the scalar field has the desired equation of state if  $V(\phi) \gg \dot{\phi}^2$ .

A discussion on which potentials can actually provide us with slow roll inflation involves the study of homogeneous classical fields in an expanding background, but the equation for this field can be derived easily. Consider an expanding sphere of volume  $V$ , in which the pressure  $P$  does work. According to the first law of thermodynamics, the change in total energy  $dE$  must be equal to the work:

$$dE = -PdV \quad (2.22)$$

But  $E = \epsilon V$ , so

$$dE = \epsilon dV + V d\epsilon = -PdV. \quad (2.23)$$

Since  $V \sim a^3$ , we can write  $dV = 3a^2 da$  and substitute in the second equality of (2.23) to obtain

$$d\epsilon = -3(\epsilon + P)\frac{da}{a}. \quad (2.24)$$

Differentiating with respect to time and substituting  $H = \dot{a}/a$ , we recoup the homogeneous, isotropic universe version of the energy conservation equation  $T_{0;\mu}^\mu = 0$ ,

namely

$$\dot{\epsilon} = -3H(\epsilon + P). \quad (2.25)$$

Thus armed with a differential equation for the energy density, we can substitute (2.20) and (2.21) in our conservation expression and obtain

$$\ddot{\phi} + 3H\dot{\phi} + \partial_{\phi}V = 0. \quad (2.26)$$

All we have left to do to, in principle, is to write  $H = \sqrt{\frac{8\pi}{3} \left( \frac{1}{2}\dot{\phi}^2 + V(\phi) \right)}$ , where we took  $G = 1$  and  $k = 0$ .

As an example, consider the simple potential  $V = \frac{1}{4}m^4\phi^4$ . This potential was chosen randomly, but as James Joyce wrote, the best things in life are random. Now, substituting, we get the closed form equation  $\ddot{\phi} + \sqrt{12\pi \left( \dot{\phi}^2 + m^4\phi^4 \right)}\dot{\phi} + m^4\phi^3 = 0$ . This does not look very friendly, but we can reduce it to a first order differential equation for  $\dot{\phi}(\phi)$ . Since  $\ddot{\phi} = \dot{\phi} \frac{d\dot{\phi}}{d\phi}$ , we could rewrite the second order equation as first order and use phase plots to study its behavior.



# Chapter 3

## Hybrid Inflation and Seeding

### 3.1 Hybrid Inflation

#### 3.1.1 Hybrid Inflation Preliminaries

We have discussed, in some manner of generality, the characteristics of inflationary mechanisms. The beauty of inflation, in a way, is how general it is. It specifies no particular Lagrangian, which is a good thing for imaginative physicist. And yet we have not attempted to draw a logical link between primordial black hole production and inflation, mostly because doing so requires both specifying Lagrangian, perhaps despite our better nature, and performing a large amount of work, much of which is still the subject of research today. Let us now try anyway, using hybrid inflation as our particular brand of inflation.

Hybrid inflation [8] differs from what we discussed in chapter 2, because it combines, along with the usual slow-roll field, a “timer” field, whose job it is to change the slow-roll field potential (we’ll call it “waterfall” field from now on) such that at some point in time the local vacuum turns into an unstable point. Thus the waterfall field “falls down” to a new minimum, where we declare inflation to end.

### 3.1.2 Hybrid Inflation Dynamics

We now have at least two fields to play with. We assume a fixed background de-Sitter space. As we have illustrated in the previous chapter, this is not a bad approximation.

The first field to consider is the slow-roll field  $\phi$ , termed “waterfall” by physicists/poets. Typically speaking in single-field inflation, the mass term in the Lagrangian would be time-independent. But as we described before, we make it explicitly time-dependent. The Lagrangian for  $\phi$  becomes[9]

$$\mathcal{L}_\phi = e^{3Ht} \left[ |\dot{\phi}|^2 - e^{-2Ht} |\nabla\phi|^2 - m_\phi^2(t) |\phi|^2 \right]. \quad (3.1)$$

Note that the exponential prefactor comes from the fact that the  $V \sim a^3$  in 3 dimensions. As well, we note that  $\phi$  must be complex, since as a single-field it is liable to creating domain walls.

To make the time-dependent mass switch sign, we use the general form

$$m_\phi^2(t) = m_0^2 \left[ 1 - \left( \frac{\psi(t)}{\psi_c} \right)^r \right], \quad (3.2)$$

where  $\psi$  is the timer field and we have chosen  $r = 4$ . The Lagrangian for  $\psi$  is

$$\mathcal{L}_\psi = \frac{1}{2} e^{3Ht} \left[ \dot{\psi}^2 - e^{-2Ht} (\nabla\psi)^2 - m_\psi^2 \psi^2 \right]. \quad (3.3)$$

Since the dynamics only care about derivatives of Lagrangian, we can add a constant  $V_0$ , which we could take to be large so that variations in  $H$  during inflation be small.

We can now express the equations of motion, in a manner similar to (2.26). For the waterfall field, we have

$$\ddot{\phi} + 3H\dot{\phi} - e^{-2Ht} \nabla^2 \phi + m_\phi^2(t) \phi = 0, \quad (3.4)$$

while the timer field behaves as

$$\ddot{\psi} + 3H\dot{\psi} - e^{-2Ht} \nabla^2 \psi + m_\psi^2 \psi = 0. \quad (3.5)$$

We do not require  $\psi$  to depend on position, so we can just as well take  $\nabla\psi = 0$ . We can then solve (3.5) if we specify as initial conditions that  $\psi(t = 0) = \psi_c$  and  $m_\phi^2(t = 0) = 0$ . We obtain:

$$\psi(t) = \psi_c e^{(-3/2 \pm \sqrt{9/4 - m_\phi^2/H^2})Ht}. \quad (3.6)$$

The form of this solution suggests rescaling the masses in the same way as time is rescaled such that the number of e-folds  $N$  is equal to  $Ht$ . We define  $\mu_\phi = m_\phi/H$  and  $\mu_\psi = \mu_\psi/H$ .

### 3.1.3 Mode Expansion

We will need to consider numerical calculations rather than analytical solutions to tackle this problem. We consider a finite cubic box of length  $b$ , whose size is measured in units of  $1/H$ , subject to periodic boundary conditions and a discrete spatial lattice with  $Q^3$  points (we go from 0 to  $Q - 1$  per dimension). Our lattice conditions become

$$\vec{x} = \frac{b}{Q} \vec{l}, \quad (3.7)$$

$$\vec{k} = \frac{2\pi}{b} \vec{n}, \quad (3.8)$$

where the vector  $\vec{l} = (l_x, l_y, l_z)$  indicate our lattice position and  $\vec{n} = (n_x, n_y, n_z)$  does the same for  $k$ -space and the integers  $n_i$  go from  $-Q/2$  to  $Q/2 - 1$ .

We can expand  $\phi$  in modes  $u(\vec{k}, t)$  in momentum space in the following way:

$$\phi(\vec{x}, t) = b^{-3/2} \sum_{\vec{k}} \left[ c(\vec{k}) e^{i\vec{k} \cdot \vec{x}} u(\vec{k}, t) + d^\dagger(\vec{k}) e^{-i\vec{k} \cdot \vec{x}} u^*(\vec{k}, t) \right], \quad (3.9)$$

where  $c(\vec{k})$  and  $d^\dagger(\vec{k})$  are the creation and annihilation operators. Going back to (3.4), we substitute in our mode expansion to get a differential equation for  $u(\vec{k}, N)$  rather than  $\phi$ :

$$\ddot{u}(\vec{k}, N) + 3\dot{u}(\vec{k}, N) + e^{-2N} \vec{k}^2 u(\vec{k}, N) - \mu_\phi^2 \left( 1 - e^{\bar{\mu}_\psi^2 N} \right) u(\vec{k}, N) = 0, \quad (3.10)$$

where we have rescaled  $\tilde{k} = |\vec{k}|/H$  and an overdot means a derivative with respect to the rescaled time  $N$ .

We can transform this equation to be explicitly in terms of the amplitude  $R(\vec{k}, t)$ , which is defined such that the solution to (3.10) is written

$$u(\vec{k}, t) = \frac{1}{\sqrt{2\tilde{k}H}} R(\vec{k}, t) e^{i\theta(\vec{k}, t)}. \quad (3.11)$$

This allows us to separate the equation in a real and an imaginary part, and we get an equation for the amplitude

$$\ddot{R} - R\dot{\theta}^2 + 3\dot{R} + e^{-2N}\tilde{k}^2 R - \mu_\phi^2 \left(1 - e^{-\tilde{\mu}_\psi^2 N}\right) R = 0. \quad (3.12)$$

This equation is coupled to  $\theta$ , which is unpleasant. We can remedy the situation by integrating the equation for the imaginary part and comparing to the early time behavior of the analytic solution (see Son). Thus uncoupled, we can rewrite (3.12) as

$$\ddot{R} + \frac{\tilde{k}^2 e^{-6N}}{R^3} + 3\dot{R} + e^{-2N}\tilde{k}^2 R - \mu_\phi^2 \left(1 - e^{-\tilde{\mu}_\psi^2 N}\right) R = 0, \quad (3.13)$$

which is the equation we tackle numerically using a fourth-order Runge-Kutta. Solving (3.13) is delicate, however, because setting up the initial conditions is non-trivial.

We know from the analytical solution at early times that  $R(N \rightarrow -\infty) \rightarrow e^{-N}$ . But we need to start numerical integration somewhere finite, and we would like to be able to do this without sacrificing too much in terms of accuracy. We therefore “refine” the far-past condition by adding extra terms  $\delta R(N)$  such that  $R(N) \equiv e^{-N} + \delta R(N)$ , and we can start integrating when the expansion starts to violate the desired accuracy bound.

We can obtain an expression for  $\delta R$  by substituting  $R(N)$  with the correction into (3.13) and then Taylor expanding. Rearranging terms, we get

$$\delta R = \mu_\phi^2 \frac{e^{2N}}{4\tilde{k}^2} \left(1 - e^{-\tilde{\mu}_\psi^2 N}\right) (\delta R + e^{-N}) - \frac{e^{-2N}}{4\tilde{k}^2} \left(\delta \ddot{R} + 3\delta \dot{R} - 2e^{-N}\right) + \frac{3}{2}\delta R^2 e^N - \frac{5}{2}\delta R^3 e^{2N} + \dots$$

We now expand  $\delta R$  in powers of  $\mu_\phi^2$  and  $e^N$  and write correction terms  $\delta R_{ij}$  as the  $i$ th order correction in  $\mu_\phi^2$  and the  $j$ th correction in  $e^N$ . We found expressions for various correction terms, up to  $\delta R_{65} = 15\mu_\phi^6 \frac{e^{5N}}{128k^6} (1 - e^{-\mu_\psi^2 N})^3$ . We also repeated this process for the phase  $\theta$ . We then plotted each term in the expansion in order to identify the smallest one, which we reserve to use as a criterion. We follow then follow the expansion until the criterion becomes larger than the accuracy bound. From there, as we discussed earlier, we can integrate to our heart's content. We have plotted  $R$  for various  $k$  and for  $\mu_\phi = 18$  and  $\mu_\psi = 1/18$  in 3-1.

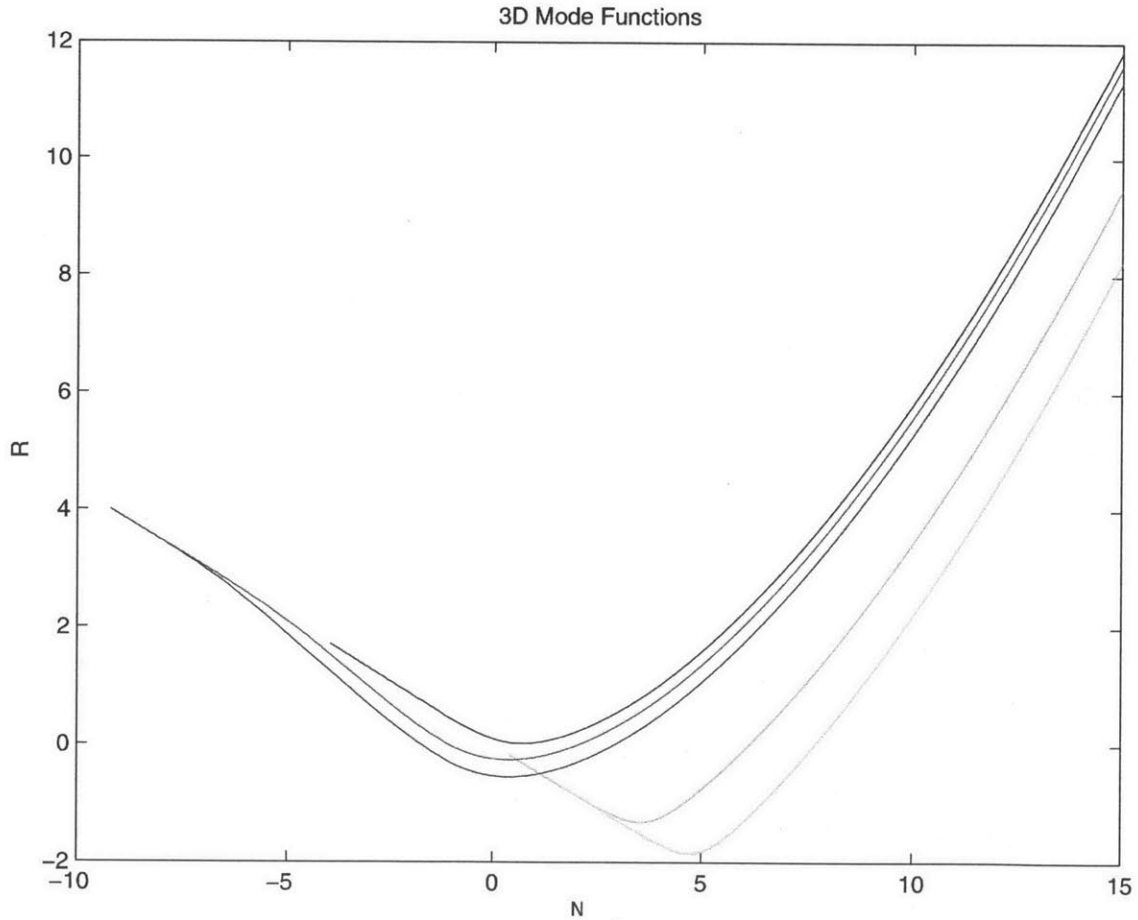


Figure 3-1: Mode functions  $R$  as a function of e-fold number, taking  $\mu_\phi = 18$  and  $\mu_\psi = 1/18$ . The pale blue is for  $k = 256$ , the green is for  $k = 64$ , the gray for  $k = 1$ , the red for  $k = 1/64$ , and dark blue for  $k = 1/256$ .

The dark blue curve represents  $k = 1/256$  and switches behavior to rapid growth

first. The other curves represent each a greater  $k$  value, up to the powder blue curve where  $k = 256$ . Note that for early times, all curves converge, which we expected, and for late time the behavior is independent of  $k$ , which we also expected.

## 3.2 Perturbations

### 3.2.1 Time Delay Formalism

The field  $\phi$  is quantum mechanical, so we expect some degree of quantum fluctuations to occur. Exactly how much depends on the inflationary model used and what it is precisely that we take to fluctuate.

For the moment, let us consider some moment, towards the end of inflation. The field rolls down towards the vacuum. Crucially, however, position-dependent perturbations to the field will lead it to reach its minimum in a given region at a slightly different time than in another region, where the perturbations are different. Because the region ends up inflating more -or less- its density will be different. The idea of a “mapping” of end-of-inflation time differences with density perturbations is called the “time-delay formalism”, and was pioneered by A. Guth. and S.Y. Pi in 1985[10]. We make abundant use of it here.

To see how this works, we make use of (2.26). The real equation of motion for the scalar field  $\phi$  has a Laplacian piece in it, but because it is multiplied by  $a^{-2} = e^{-2N}$  it becomes negligible at late times. Let the classical homogeneous solution to  $\phi$  be  $\phi_0(t)$  and write the full solution as the sum of the classical part and a small, space-dependent perturbation  $\delta\phi(\vec{x}, t)$ , i.e.

$$\phi(\vec{x}, t) = \phi_0(t) + \delta\phi(\vec{x}, t). \quad (3.14)$$

We then substitute this expression into our equation of motion. To first order in  $\delta\phi$ , we get

$$\delta\ddot{\phi} + 3H\delta\dot{\phi} + \frac{\partial^2 V}{\partial\phi_0^2}\delta\phi. \quad (3.15)$$

We can also take the time derivative of the equation of motion for  $\phi_0$  to get

$$\delta\ddot{\phi}_0 + 3H\delta\ddot{\phi}_0 = -\frac{d}{dt}\frac{\partial V}{\partial\phi} = -\frac{\partial\phi}{\partial t}\frac{d}{d\phi}\frac{\partial V}{\partial\phi} = \frac{\partial^2 V}{\partial\phi_0^2}\dot{\phi}_0, \quad (3.16)$$

which means that  $\delta\phi$  and  $\dot{\phi}_0$  follow the same differential equation. By analogy to a spring, we also see that the presence of a “damping term” implies that at late times,  $\delta\phi \propto \dot{\phi}_0$ , so we write

$$\delta\phi(\vec{x}, t) = \delta\tau(\vec{x})\dot{\phi}_0. \quad (3.17)$$

This is almost what we want. We finally take this expression to first order in  $\delta\tau$  and find that

$$\phi(\vec{x}, t) \rightarrow \phi_0(t - \delta\tau(\vec{x})). \quad (3.18)$$

This result is quite powerful. It means that our quantum field  $\phi$ , at late times, behaves like the homogeneous classical solution, up to a time offset which depends on position.

### 3.2.2 Direct Integration Method

In the literature, most calculations of density perturbations have involved further numerical calculations, usually of the Monte Carlo type. The M.I.T. hybrid inflation group, made of Alan Guth, Evangelos Sfakianakis, Illan Halpern, Matthew Joss, and the author, has been working since Summer 2012 on developing an alternative that does not require a classical trajectory.

As a first step, recall that that the mode functions, for late times, all behave similarly and exponentially in time. We write formally that

$$u(\vec{k}, t \rightarrow \infty) \sim e^{\lambda t}u(\vec{k}), \quad (3.19)$$

where  $u(\vec{k})$  does not depend on time. To find  $\lambda$ , we go back to (3.13) and assume that  $\tilde{\mu}_\psi$  is small and that  $N$  is large but not enough to completely cancel the last

term on the right. We cancel the dependence on  $\tilde{k}$  and get

$$\ddot{R} + 3\dot{R} - \mu_\phi^2 \left(1 - e^{-\tilde{\mu}_\psi^2 N}\right) R = 0. \quad (3.20)$$

Because of the slow exponent multiplying the  $R$  term, we treat it as a constant and solve (3.20) as a linear, homogeneous second order differential equation using the model solution  $R(N) = R_0 e^{\lambda N}$ , which yields

$$\lambda = -\frac{3}{2} + \frac{1}{2} \sqrt{9 + 4\mu_\phi^2 \left(1 - e^{-\tilde{\mu}_\psi^2 N}\right)}, \quad (3.21)$$

where we have neglected the negative solution because it only remains real for small  $\mu_\phi$ .

We care about the end of inflation, however, so the exponential part grows larger and more negative for larger  $N$ , which results in

$$\lambda_0 = -\frac{3}{2} + \frac{1}{2} \sqrt{9 + 4\mu_\phi^2}. \quad (3.22)$$

Now, we need to define a few quantities of importance. We define

$$\phi_{rms} \equiv \sqrt{\langle 0 | \phi(x, t) \phi^*(x, t) | 0 \rangle} \quad (3.23)$$

as the root mean square value of the waterfall field, evaluated on the Bunch-Davis vacuum. The use of this vacuum state is justified, because we assume the interaction of cosmological perturbations are strong enough to drive excited states towards the vacuum. To be absolutely sure, we would need to actually calculate decay rates and show that they are not too suppressed by the Planck mass or a slow-roll parameter. We make no attempt whatsoever at proving this and instead motor on with the Bunch-Davis vacuum.

We now insist on defining the end  $t_0$  of inflation as the moment where  $\phi_{rms}$  reaches



$\phi_{end}$ . Since all late modes more or less grow at the same exponential rate, we find

$$\phi_{rms}^2(t_0) = |\phi(\vec{x}, t_0)|^2 e^{2\lambda\delta t}. \quad (3.24)$$

We can solve for the time delay and rescale by the rms field  $\tilde{\phi}(\vec{x}, t) \equiv \frac{\phi(\vec{x}, t)}{\phi_{rms}}$  to obtain

$$\delta t(\vec{x}) = -\frac{1}{2\lambda} \ln |\tilde{\phi}(\vec{x}, t)|^2. \quad (3.25)$$

From here, we write the two-point function, which is the Fourier transform of the power spectrum, as

$$\langle \delta t(\vec{x}) \delta t(\vec{0}) \rangle = \frac{1}{4\lambda^2} \langle \ln |\tilde{\phi}(\vec{x}, t_0)|^2 \ln |\tilde{\phi}(\vec{0}, t_0)|^2 \rangle. \quad (3.26)$$

Next, we decompose  $\tilde{\phi}(\vec{x}, t) = X_1 + iX_2$  and  $\tilde{\phi}(\vec{0}, t) = X_3 + iX_4$ , where the  $X$ s are real. Since we have, in this case, a free field theory, we take the  $X$ s to be random variables in position following a jointly Gaussian distribution, where the probability density is

$$p(X) = \frac{1}{4\pi^2 \sqrt{\det(\Sigma)}} \exp\left(-\frac{1}{2} X^T \Sigma^{-1} X\right), \quad (3.27)$$

where  $\Sigma_{ij}$  is the correlation matrix  $\langle X_i X_j \rangle$ . Our two-point function therefore becomes, in this language of jointly-Gaussian distributions,

$$\langle \delta t(\vec{x}) \delta t(\vec{0}) \rangle = \int \prod_{i=1}^4 \frac{\ln(X_1^2 + X_2^2) \ln(X_3^2 + X_4^2)}{16\pi^2 \lambda^2 \sqrt{\det(\Sigma)}} \exp\left(-\frac{1}{2} X^T \Sigma^{-1} X\right) dX_i. \quad (3.28)$$

This looks somewhat promising, but we have yet to evaluate  $\Sigma = \langle XX \rangle$ . To do so, we go back to (3.9) and use the commutation relations for the creation and annihilation operators and work out the expectation values, which turn out to be

$$\Sigma = \begin{bmatrix} \frac{1}{2} & 0 & \Delta & 0 \\ 0 & \frac{1}{2} & 0 & \Delta \\ \Delta & 0 & \frac{1}{2} & 0 \\ 0 & \Delta & 0 & \frac{1}{2} \end{bmatrix}, \quad (3.29)$$

where  $\Delta = \frac{1}{2b^3} \sum_{\vec{k}} \left| \frac{u(\vec{k}, t)}{\phi_{rms}(t)} \right|^2 e^{i\vec{k} \cdot \vec{x}}$ .

To ease our way in evaluating the integral, we use polar coordinates variables  $(r_i, \theta_i)$  such that  $X_1 = r_1 \cos \theta_1$ ,  $X_2 = r_1 \sin \theta_1$ ,  $X_3 = r_2 \cos \theta_2$ , and  $X_4 = r_2 \sin \theta_2$ . Further, we change the angular variables to  $\theta = \theta_1 - \theta_2$  and  $\tilde{\theta} = \theta_1 + \theta_2$ , and the radial variables  $r_1 = r \cos \phi$  and  $r_2 = r \sin \phi$ .

This gerrymandering of the variables was not for show. Let's see what we get:

$$\langle \delta(\vec{x}) \delta t(\vec{0}) \rangle = \frac{1}{\pi \lambda^2 (1 - 4\Delta^2)} \int_0^{2\pi} d\theta \int_0^{\pi/2} d\phi \sin(2\phi) \int_0^\infty r^3 \ln(r \cos \phi) \ln(r \sin \phi) \exp \left[ -\frac{r^2 (1 - 2\Delta \sin(2\phi) \cos \theta)}{1 - 4\Delta^2} \right] dr. \quad (3.30)$$

Lo and behold, we have managed to find a way to separate the radial integration. Even better, however, is the fact that it can be done analytically:

$$\int_0^\infty r^3 \ln(r \cos \phi) \ln(r \sin \phi) e^{-\alpha r^2} dr = \frac{1}{8\alpha^2} \left[ (\gamma - 2)\gamma + \pi^2/6 - 2 \ln(\cos \phi \sin \phi) (\gamma - 1 + \ln \alpha) + 4 \ln(\cos \phi) \ln(\sin \phi) \right], \quad (3.31)$$

where  $\gamma \approx 0.58$  is Euler's constant and  $\alpha = \frac{1 - 2\Delta \cos \theta \sin(2\phi)}{1 - 4\Delta^2}$ . This is a fantastic result, because we have reduced the problem to integrating over 2 variables, from our initial 4.

### 3.2.3 Results

While we are able to graph the two-point function directly, of more immediate interest to primordial black hole seeding is its Fourier transform, namely the power spectrum

$$\delta\tau(\vec{k}) \equiv \left[ \frac{k^3}{8\pi^3} \int \langle \delta t(\vec{x}) \delta t(\vec{0}) \rangle e^{i\vec{k} \cdot \vec{x}} d\vec{x} \right]^{1/2}. \quad (3.32)$$

We graph the power spectrum for mass parameters  $\mu_\phi = 20$  and  $\mu_\psi = 1/20$ .

The reason for this relevance is that most sources in the literature relate conditions for primordial black hole production directly to the curvature power spectrum. Indeed

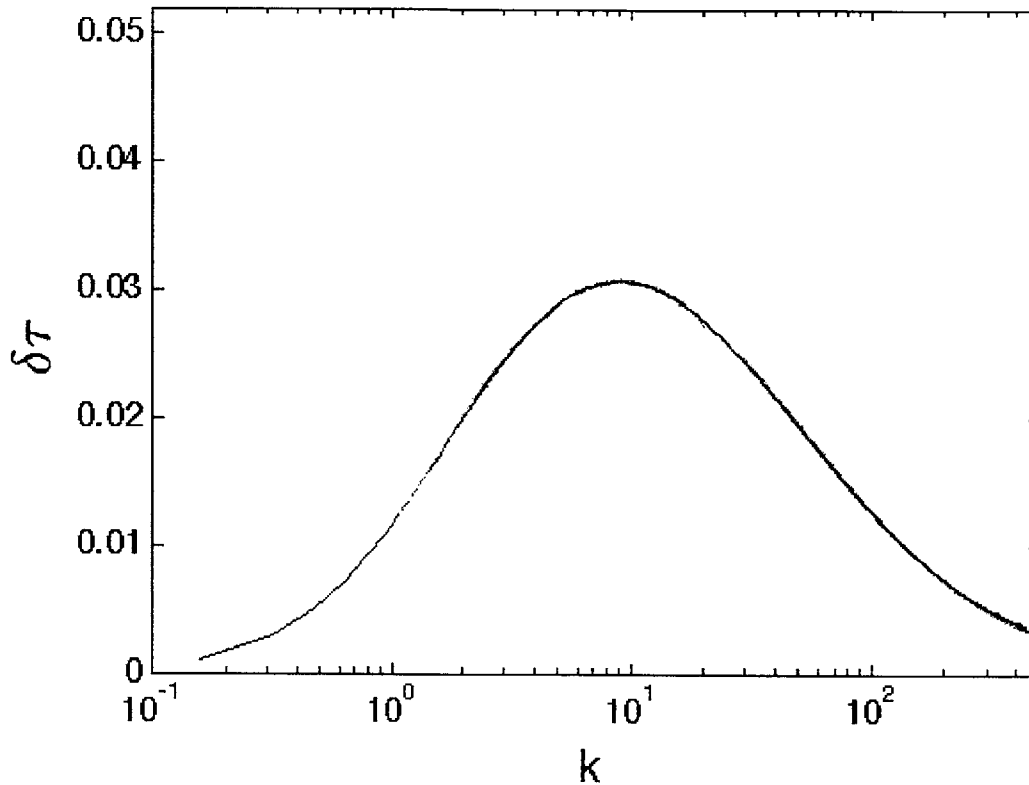


Figure 3-2: This plot was adapted, with permission, from a plot produced by Evangelos Sfakianakis. Graphed is the  $\tau$  spectrum, as a function of  $k$  in Hubble units. Note the presence of a peak at around  $k = 10$ .

it seems that, regardless of the particular flavor of inflation used, most authors agree that some bounds on the curvature power spectrum are required in order to produce primordial black holes.

Cosmologists, like David Lythe[11] who has worked extensively on related topics, often quote Bernard Carr's 1975 paper[12] on the primordial black hole mass spectrum as a starting point. Of course, this was written in the pre-inflation era, without the subtleties of hybrid inflation in mind.

The author has spent a considerable amount of time trying to adapt Carr's ideas, as Lythe and Takayama[13] have done in their own specific situations, to the specifics of our formalism. The results were unsuccessful.

On the one hand, we can adapt the requirements that overdense regions, which

we take to be spherical, have larger density than a critical value and constrain

$$\sqrt{\delta_0} \frac{a_0}{t_0} > \sqrt{f}, \quad (3.33)$$

where  $\delta_0$  is the initial density contrast upon horizon re-entry, and  $t_0$  and  $a_0$  correspond to the time and scale factor at that moment, while  $P = f\mu$  is the equation of state (which may change with time). We can therefore estimate that the curvature perturbations  $\mathcal{R}_0$  need to be at least of order unity, since  $f$  is.

This argument, however, is not foolproof. At the same time, we have not been able to address the outer bound, namely the bound required to not produce a separate universe. Takayama writes a condition based on bounds on the radial derivative of  $\mathcal{R}$ , but we have not managed to reverse-engineer its origins so as to see if we could adapt it to our own purposes. All in all, what we are left with from the literature is the notion that we need a peak in the curvature spectrum. This peak is found by Takayama to be around  $k = 810 \text{ Mpc}^{-1}$ , but in the absence of greater insight as to when the appropriate modes re-enter the horizon and condensate critically, we cannot provide a scale to our  $k$  values, which are measured in units of  $H$ .

# Bibliography

- [1] P. Schechter, *Astrophys. J.* **203**, 297 (1976).
- [2] S. Chandrasekhar, *Phys. Rev. Lett.* **12**, 114 (1964).
- [3] M. S. Clemens, M. Negrello, G. De Zotti, J. Gonzalez-Nuevo, L. Bonavera, G. Cosco, G. Guarese and L. Boaretto *et al.*, arXiv:1305.1647 [astro-ph.GA].
- [4] T. W. B. Kibble, *J. Phys. A* **9**, 1387 (1976).
- [5] Y. B. Zeldovich and M. Y. Khlopov, *Phys. Lett. B* **79**, 239 (1978).
- [6] J. Preskill, *Phys. Rev. Lett.* **43**, 1365 (1979).
- [7] A. H. Guth, *Phys. Rev. D* **23**, 347 (1981).
- [8] A. D. Linde, *Phys. Rev. D* **49**, 748 (1994) [astro-ph/9307002].
- [9] A. H. Guth and E. I. Sfakianakis, arXiv:1210.8128 [astro-ph.CO].
- [10] A. H. Guth and S. -Y. Pi, *Phys. Rev. D* **32**, 1899 (1985).
- [11] D. H. Lyth, arXiv:1107.1681 [astro-ph.CO].
- [12] B. J. Carr, *Astrophys. J.* **201**, 1 (1975).
- [13] M. Kawasaki, T. Takayama, M. Yamaguchi and J. 'i. Yokoyama, *Phys. Rev. D* **74**, 043525 (2006) [hep-ph/0605271].